Concentrating immiscible molecules at solid@MOF interfacial nanocavities to drive an inert gas-liquid reaction at ambient conditions

Sim, Howard Yi Fan; Lee, Hiang Kwee; Han, Xuemei; Koh, Charlynn Sher Lin; Phan-Quang, Gia Chuong; Lay, Chee Leng; Kao, Ya-Chuan; Phang, In Yee; Yeow, Edwin Kok Lee; Ling, Xing Yi

2018

Sim, H. Y. F., Lee, H. K., Han, X., Koh, C. S. L., Phan-Quang, G. C., Lay, C. L., Kao, Y. C., Phang, I. Y., Yeow, E. K., & Ling, X. Y. Concentrating immiscible molecules at solid@MOF interfacial nanocavities to drive an inert gas-liquid reaction at ambient conditions. Angewandte Chemie International Edition. doi:10.1002/anie.201809813

https://hdl.handle.net/10356/80453

https://doi.org/10.1002/anie.201809813

SUPPORTING INFORMATION

Table of Contents

SUPPORTING INFORMATION

Experimental Procedures

Chemicals

Silver nitrate (≥ 99 %), anhydrous 1,5-pentanediol (PD, ≥ 97 %), poly(vinylpyrrolidone) (PVP, average MW = 55,000), decane (≥ 98 %), aniline (ACS reagent, ≥ 99.5 %), zinc nitrate hexahydrate (reagent grade, 98 %), 2-methylimidazole (99 %), 1H,1H,2H,2H-perfluorodecanethiol (PFDT; 97 %) and tetraethyl orthosilicate (99.999 % trace metals basis) were purchased from Sigma Aldrich; copper (II) chloride (≥ 98 %) was from Alfa Aesar; methanol (ACS reagent, ≥ 99.8 %) was from J.T.Baker®; ethanol (ACS, ISO, Reag. Ph Eur) and ammonia (ACS, Reag. Ph Eur) was from EMSURE®; dimethylformamide (HPLC grade) was obtained from Fisher Scientific; nitrogen (N_2; ALPHAGAZ 1; 99.999 %) and carbon dioxide (CO_2; ALPHAGAZ 1; 99.99 %) were purchased from Singapore Oxygen Air Liquide Pte Ltd. All chemicals were applied without further purification. Milli-Q water (> 18.0 MΩ. cm) was purified with a Sartorius Arium® 611 UV ultrapure water system.

Synthesis and purification of silver nanocubes

The preparation of Ag nanocubes were synthesized of high yield via polyol method described in literature.[1] Briefly, 10 mL of copper (II) chloride (8 mg/mL), poly(vinylpyrrolidone) (20 mg/mL) and silver nitrate (20 mg/mL) were separately dissolved in 1, 5-pentanediol. The chemicals were sonicated and vortexed repeatedly to dissolve them. 35 µL copper (II) chloride solution was then added to the silver nitrate solution. Then, 20 mL 1, 5-pentanediol in a 100 mL round bottomed flask was heated to 190 ^{o}C for 10 min. 250 µL poly(vinylpyrrolidone) precursor was added to flask dropwise every 30 s while 500 µL silver nitrate precursor was injected every min using a quick addition. The addition process continued until the greenish coloration of the reaction mixture faded off.

For the purification of Ag nanocubes, 1, 5-pentanediol was first removed from the mixture through centrifugation. The Ag nanocubes solution was then dispersed in 10 mL ethanol and 100 mL aqueous poly(vinylpyrrolidone) solution (0.2 g/L). The resulting solution was vacuum filtered using Durapore® polyvinylidene fluoride filter membranes (Millipore) with pore sizes ranging from 5000 nm, 650 nm, 450 nm and 220 nm, repeated several times for each pore size. The Ag nanocubes were then redispersed in ethanol (10 mg/mL) and stored in fridge.

Assembly of Ag nanocubes via Langmiur-Blodgett method

The preparation of Ag nanocubes assembled on Si substrates were prepared as described in literature.[2] Briefly, Si (100) substrates were cleaned prior to assembly of Ag naocubes using oxygen plasma (FEMTO SCIENCE, CUTE-MP/R, 100 W) for 5 min. The surface pressure was zeroed before addition of PVP-caped Ag nanocubes. 700 µL of the ethanolic purified Ag nanocubes was dispersed in 1050 µL of chloroform and then added carefully to the surface of the water in the Langmiur-blodgett trough (KSV NIMA, KN1002). The surface pressure can be tuned by moving the mechanical barrier of the machine. Surface pressure of 16 mN/m were employed, and the pull rates and compression rate were fixed at 2 mm/s.

1H,1H,2H,2H-perfluorodecanethiol (PFDT) functionalization of Ag nanocubes

The removal of surfactant from Ag nanocubes surface was done by functionalizing the assembled Ag nanocubes with PFDT. The assembled Ag nanocube array was immersed in 5 mM of PFDT methanolic solution for at least 15 hours.

SUPPORTING INFORMATION

Growth of Zeolitic Imidazolate Framework – 8 (ZIF) film on PFDT-capped Ag nanocubes array

ZIF film was grown on the nanocubes array using a procedure reported from literature.[3] 2 ml of methanolic $Zn(NO_3)_2$ (25 mM) was added to 2 ml of methanolic 2-methylimidazole (mIM; 50 mM) and mixed quickly for 5 s. For one growth cycle, the PFDT-capped Ag nanocubes substrate was immersed in the solution for 40 minutes, and then washed with copious amount of methanol and dried with nitrogen gas several times to remove excess ZIF crystals. The procedure was repeated 2 more times using fresh $Zn(NO_3)_2$ and 2-methylimidazole solutions to obtain ZIF film of increasing thickness.

Activation of Ag@ZIF substrate

The Ag@ZIF substrates were thermally activated to remove any solvent molecules within its pores by heating the substrate under vacuum at 120ºC for 2 hours. The substrates were used immediately after activation.

Synthesis of Ag@ZIF core-shell

250 µL of $Zn(NO_3)_2$ (25 mM) was added to a vial of 1.3 mL methanol and stirred at 500 rpm for 5 minutes. 250 µL of methanolic 2-methylimidazole (50 mM) was then added, followed by the immediate addition of 200 µL Ag nanocubes solution (4.7 mg/mL). The mixture was stirred for another 90 minutes at 500 rpm. Excess reagents were removed by centrifugation and the core-shell nanoparticles were then washed twice with methanol and then finally re-dispersed in methanol.

Synthesis of silica beads

Silica beads were synthesized using a modified Stober process. 1500 µL of pure water and 1500 µL of ammonia were added dropwise into 760 µL of tetraethylorthosilicate ethanolic solution (0.35 M) respectively under vigorous stirring for 30 mins. The water-soluble silica beads were then washed with ethanol and water and subsequently redispersed in methanol.

Synthesis of SiO_2@ZIF core-shell

250 µL of $Zn(NO_3)_2$ (25 mM) was added to a vial of 1.3 mL methanol and stirred at 500 rpm for 5 minutes. 250 µL of methanolic 2-methylimidazole (50 mM) was then added, followed by the immediate addition of 200 µL SiO_2 nanospheres solution (4.7 mg/mL). The mixture was stirred for another 90 minutes at 500 rpm. Excess reagents were removed by centrifugation and the core-shell nanoparticles were then washed twice with methanol and then finally re-dispersed in methanol.

SERS evaluation

The thermal-activated platforms were placed inside a custom-made gas flow cell for SERS examination. The gas flow cell was first flushed with N_2 gas (5 sccm) for 30 min to displace air from our experimental set-up. Following which, CO_2 gas (5 sccm) was flown through the gas flow cell and SERS analysis was performed in-situ for a duration of 90 min. Subsequent purging of the experimental set-up with N_2 gas and simultaneous SERS analysis were conducted until characteristic SERS bands remain constant in the SERS spectra (30 min). All gas flows were precisely controlled using precision gas mass flow controllers (model number MC-100SCCM-D) obtained from

Alicat Scientific, Inc. All SERS spectra were normalized between 0 (min) and 1 (max) and their SERS intensities (I) were based on the relative intensity on respective SERS bands.

Density functional theory (DFT) simulation

The calculation on the interaction of Ag surface with possible products were carried out using the unrestricted B3LYP exchange-correlation functional, as implemented in the Gaussian 09 computational chemistry package. The 6-31g (d p) basis set was used for all atoms except Ag, for which the LANL2DZ basis set was employed. The Ag surface was modelled using a reported triangle consisting of 6 Ag atoms.[4] After geometry optimization of the triangular Ag cluster, possible product molecule was then placed near the Ag cluster (< 2 Å) and the entire system was re-optimized. ZIF was excluded from the simulation owing to its nanoscopic separation from the SERS-active surface, as demonstrated experimentally via the lack of ZIF's vibrational features during SERS evaluations.

Ex-situ UV-Vis reaction monitoring

Solid@ZIF core-shell nanoparticles were dispersed in 1.3 mL aniline/decane mixture (0.1 M) solution. The gas flow cell was first flushed with N_2 gas (5 sccm) for 30 min to displace air from our experimental set-up. Following which, CO_2 gas (5 sccm) was introduced through the gas flow cell and UV-Vis analysis was performed at pre-defined timings of 0, 30, 60, 120, 150, 180, 240 and 360 min for UV-vis measurements to quantify the concentration of aniline. The apparent rate constant (*k*) can be determined based on the multiplication between the concentration of the reaction medium and the gradient of the C/C_o plot exhibited by solid@ZIF and ZIF.

Characterization

Scanning electron microscope (SEM) imaging was performed using JEOL-JSM-7600F microscope. Transmission electron microscope (TEM) imaging was performed using JEOL-2100 at an accelerating voltage of 200 kV. UV-vis spectra were measured with Cary 60 UV-vis spectrometer. Substrate X-ray diffraction patterns were recorded on a Bruker GADDS XRD diffractometer with Cu Ka radiation. SERS measurements were performed using x-y hyperspectral imaging mode of the Ramantouch microspectrometer (Nanophoton Inc., Osaka, Japan) with an excitation wavelength of 532 nm and laser power of 0.07 mW. A 50× objective lens (N.A. = 0.55) with 5 s acquisition time was used for data collection. All SERS spectra were obtained by averaging the individual SERS spectra within the SERS image.

Supporting Figures and Notes

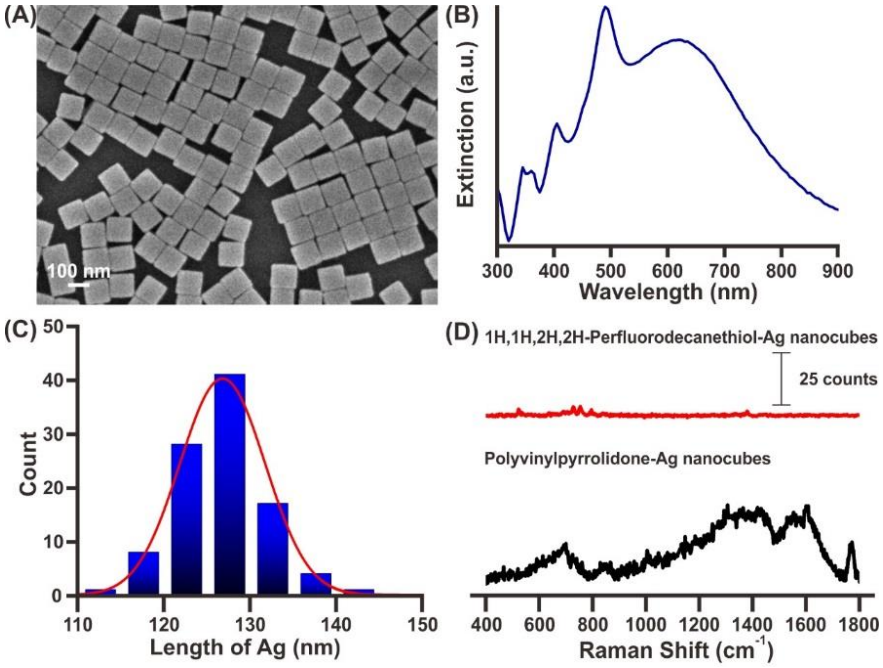

Figure S1. Characterization of PFDT-functionalized Ag nanocubes. (A) SEM image of PFDT-functionalized Ag nanocubes. (B) Extinction spectrum of PFDT-functionalized Ag nanocubes. The peaks at 348, 412, 525 and 674 nm can be assigned to octupole (348 nm), quadrupole (412 nm and 525 nm), and dipole resonances (674 nm), respectively. (C) Size distribution of Ag nanocubes. (D) SERS spectra of PFDT-functionalized compared to PVP coated Ag nanocubes.

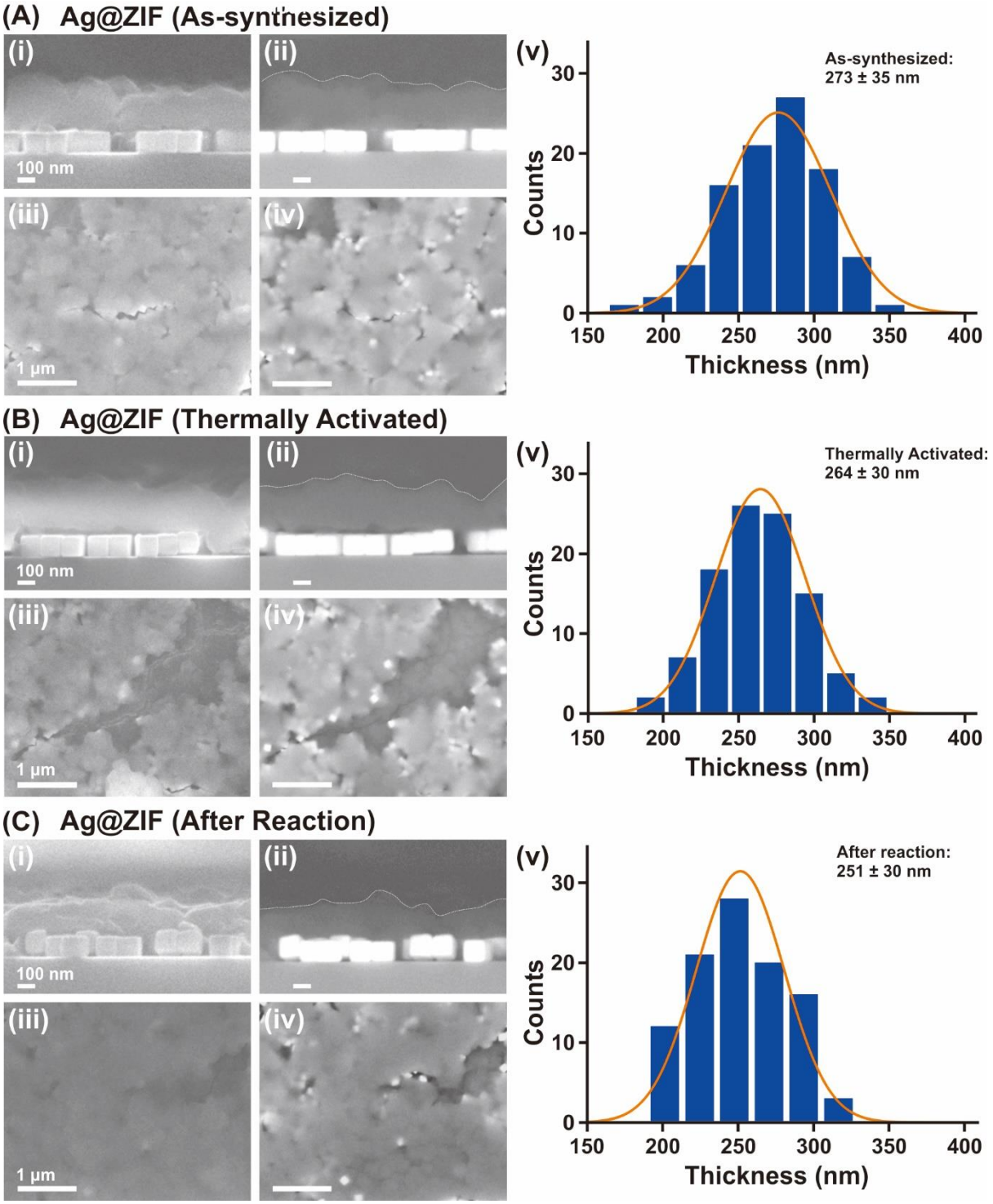

Figure S2. Characterization of Ag@ZIF before and after reaction. (A) As-synthesized Ag@ZIF, (B) Thermally activated Ag@ZIF and (C) Ag@ZIF after reaction. (i-ii) Cross-sectional SEM images in SEI and LABE modes respectively. (iii-iv) Top view SEM images in SEI and LABE modes respectively. (v) ZIF thickness distribution.

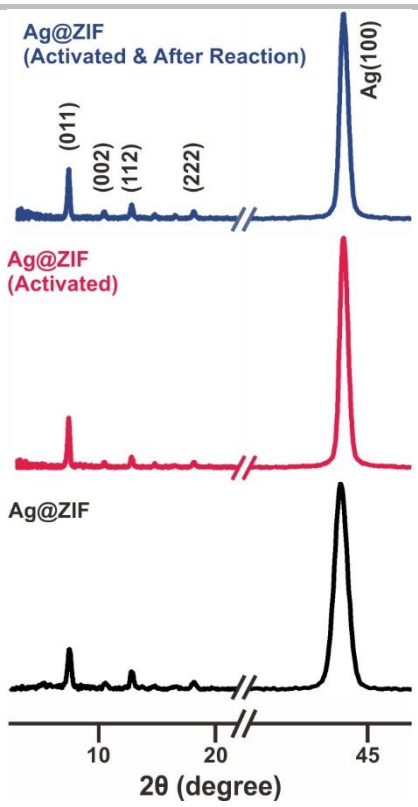

Figure S3. Substrate XRD diffraction pattern of as-synthesized Ag@ZIF, thermally activated Ag@ZIF and thermally activated Ag@ZIF after reaction (from bottom to top). XRD patterns at 7.5, 10.5, 12.8 and 18.0° coincide with ZIF's (011), (002), (112) and (222) facets,[5] respectively. XRD peak at 44.4° can be indexed to the (100) facet of single crystalline Ag nanocube.[6]

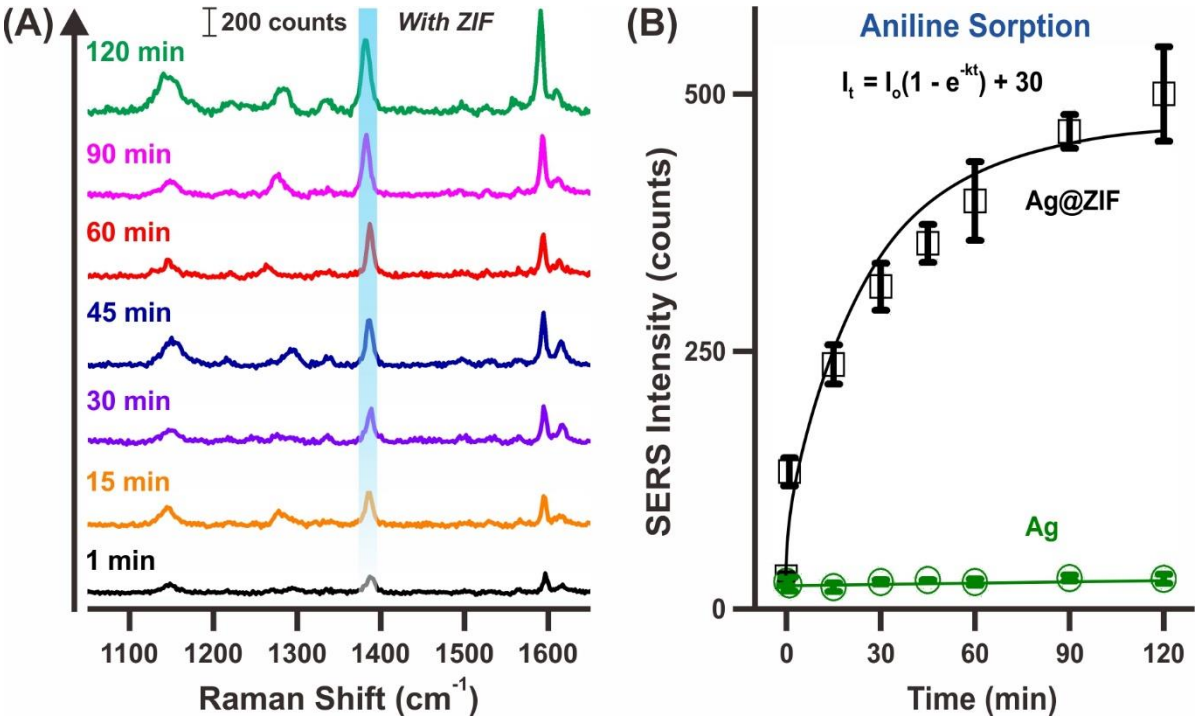

Figure S4. Time-dependent aniline concentrating effect in Ag@ZIF over 2 hrs. (A) SERS spectra under N_2 flushing. (B) SERS intensity measurement of aniline sorption comparing with (black) and without (green) ZIF film.

Ag@ZIF intensity-time plot can be fitted using a Lagergren pseudo first order adsorption kinetics (Figure S4) based on linear driving force model, which follows the equation: $I = I_{max}(1\text{-}e^{-kt}) + 30$ where I is the time-dependent SERS intensity (in counts) at time t, I_{max} the final equilibrium intensity and k (s^{-1}) gives the pseudo first-order adsorption rate constant. Notably, Ag@ZIF rate constant 37.5 ms^{-1} exhibits a sharp increase in intensity within the first 1 min which further reflects advantage of ZIF in enabling swift capturing and enriching of the analyte molecules. The Ag control platform remain constant throughout the experiment due to absence of ZIF concentrating effect.

Our experimental SERS peaks at 1594 and 1615 cm^{-1} are indexed to the combination of NH_2 bending and aromatic ring stretching ($\delta_{NH2} + \nu_{CC}$) and a combination of CN stretching, NH_2 bending and aromatic ring stretching ($\nu_{CN} + \delta_{NH2} + \nu_{CC}$) of aniline, respectively. Both peaks exhibit common unique vibrational modes involving NH_2 bending of aniline and aromatic ring stretching ($\delta_{NH2} + \nu_{CC}$). With increasing of time, there is a continuous accumulation of analyte (aniline) molecules close to the SERS-active Ag nanocube surfaces (analyte concentrating effect of ZIF). The enrichment of aniline in the interfacial cavities could influence the orientations and interactions of these molecules with each other and/or the Ag surfaces. Therefore, as molecules are concentrated within the interfacial cavities from t = 45 to 90 min, we note a slight change in the SERS intensity ratio of the vibrational modes at 1594 and 1615 cm^{-1} as a result of varying molecular environment in the interfacial cavities.[3,7] Consequently, such intensity ratio variation could result in an apparent increase of the 1615 cm^{-1} band intensity at t = 45 min, which subsequently reduces beyond t = 60 min.

Nevertheless, both the time-dependent increase in SERS intensity of 1387 cm^{-1} band (Figure S4B) and the overall SERS spectra (Figure S4A) evidently demonstrate the swift molecular concentrating effect enabled by Ag@MOF system.

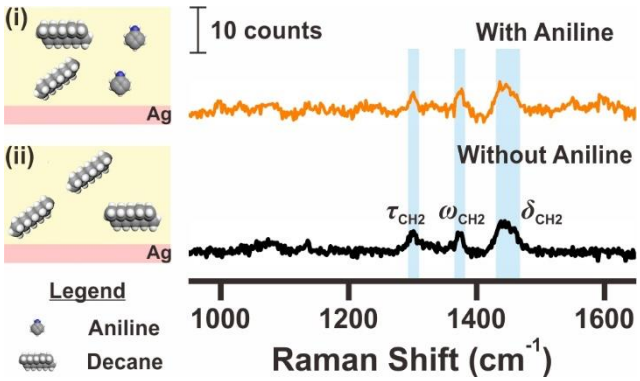

Figure S5. Control experiments using Ag platform for detection in aniline/decane mixture (i) with aniline and (ii) without aniline.

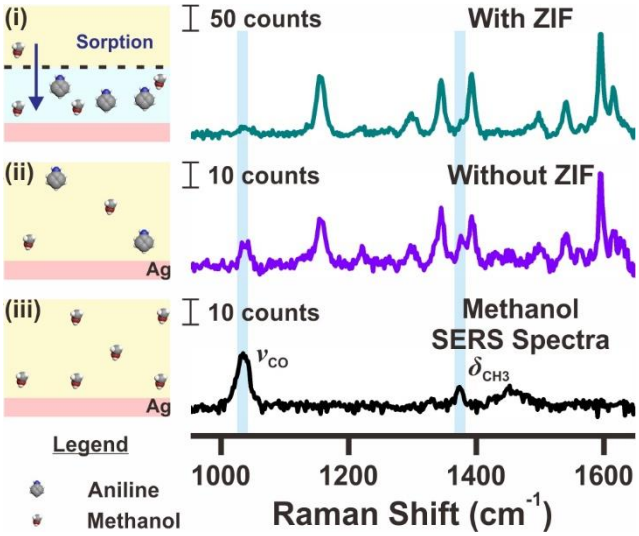

Figure S6. Molecule size selectivity in aniline/methanol mixture (i) with ZIF, (ii) without ZIF and (iii) SERS spectra of methanol.

We highlight the importance of selecting an ideal solvent for our experimental setup by choosing small molecule solvent such as methanol which is undesirable as it will compete for sorption into interfacial cavities and post spectra interferences. Similarly, we immerse our Ag@ZIF substrate into 0.1 M aniline/methanol mixture and monitor the capturing of methanol (3.6 Å) and aniline (~5.9 Å) via SERS detection.[8-9] Our SERS spectra reveal the emergence of two additional peaks at 1032 and 1375 cm^{-1} (Figure S6-i), which can be indexed to (ν_{CO}) and (δ_{CH2}) modes of methanol (Figure S6-iii),[9] respectively. This indicates the diffusion of methanol into ZIF's pores hence causing spectra interference. Notably, we notice weak intensity SERS bands of aniline and methanol simultaneously in the absence of ZIF (Figure S6-ii). Thus, this further emphasize on the importance of integrating ZIF onto Ag to concentrate and enrich liquid molecules near Ag surface for detection.

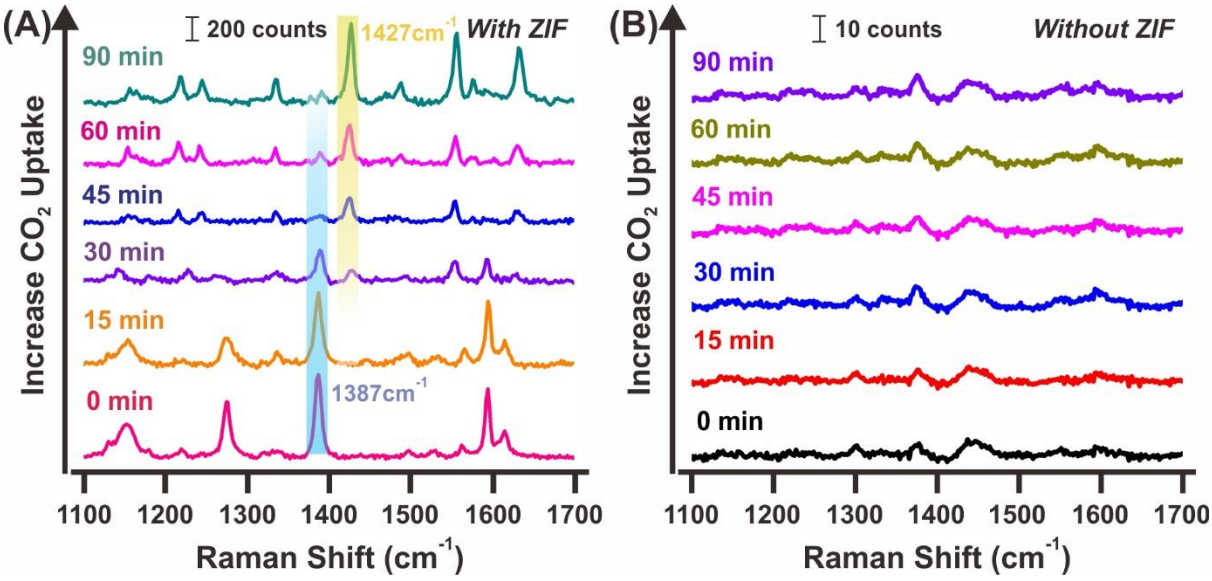

Figure S7. Time-dependent SERS spectra of reaction over 90 min (A) with ZIF and (B) without ZIF.

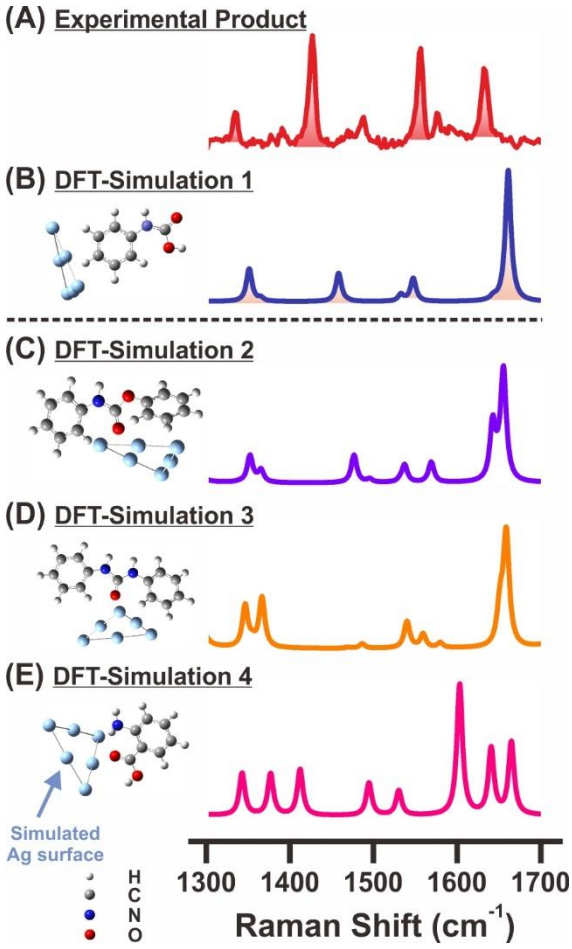

Figure S8. Overview DFT-simulated Raman spectra of possible products with Ag 6 cluster. (A) Experimental product, (B) phenylcarbamic acid, (C) phenyl phenylcarbamate, (D) 1,3-diphenylurea and (E) 2-aminobenzoic acid.

The simulated aniline SERS bands at 1363 and 1540 cm^{-1} are attributed to ρNH_2 and vCN, respectively. These SERS bands exhibit lower intensity compared to the experimental spectra of aniline due to the following possible reasons: (1) There could be a difference between the experimental aniline structure/orientation near the plasmonic nanocubes as compared with our simulated Ag_6-aniline model. (2) Our single molecule simulation does not account for the overall coverage effects of multiple aniline molecules near the plasmonic nanocubes, possibly resulting in the slight discrepancies between the experimental and DFT SERS intensities.[12-13] Nevertheless, our experimental peaks at 1387 and 1562 cm^{-1} are indeed indexed to ρNH_2 and vCN, respectively, as supported by qualitative comparisons with DFT-simulated results and reported literatures.[11]

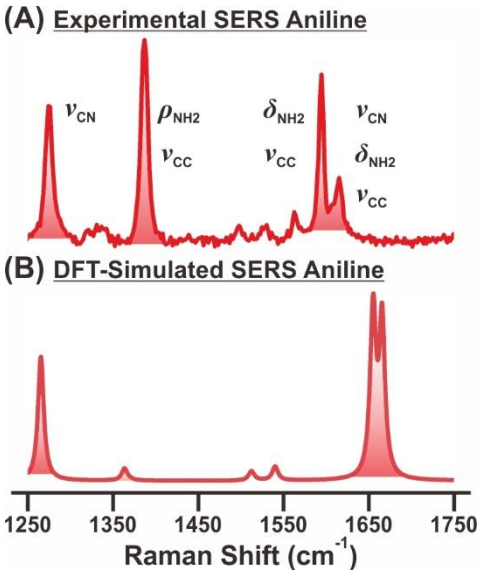

Figure S9. Overview SERS spectra of aniline in comparison to DFT-simulation.

Both our aniline SERS spectra and literature studies are in agreement with our DFT simulated spectra (Figure S9; Table S1),[11] which validates the accuracy of using the method for subsequent simulations. The red shift in the experimental vibrational peaks at 1594 and 1615 cm^{-1} from the simulated SERS peaks at 1654 and 1665 cm^{-1} is possibly due to the differences in molecule structure orientation and single molecule does not serve the effect of multiple molecules near Ag.[12-13] Nevertheless, with our simulation, the former vibration (1594 cm^{-1}) can be assigned to (δ_{NH2} + ν_{CC}) while the latter (1615 cm^{-1}) is indexed to (δ_{NH2} + ν_{CN} + ν_{CC}) where similar vibrations are observed in previous study.

Table S1. SERS vibrational modes of aniline and their band assignments.

Experimental (cm^{-1})	Simulated Aniline (cm^{-1})	Assignment
1274	1265	ν(C–N) + δ(C–H)
1387	1363	ρ(NH_2) + ν(C–C) + δ(C–H)
1562	1540	ν(C–N) + ν(C–C) + δ(C–H)
1594	1654	δ(NH_2) + ν(C–C) + δ(C–H)
1615	1665	δ(NH_2) + ν(C–N) + ν(C–C) + δ(C–H)

ν, stretching; δ, in-plane deformation; ρ, rocking

Table S2. DFT-Simulated SERS vibrational modes of phenylcarbamic acid and their band assignments.

Experimental (cm^{-1})	Simulated Phenylcarbamic acid (cm^{-1})	Assignment
1335	1351	ν_{as}(C=C–N) + ν(N–C=O) + aromatic ring stretch
1427	1458	ν_{as}(N−C−OH) + δ(C–O–H) + ν(C=O) + aromatic ring stretch
1556	1547	ν_{as}(C–N–C) + ν(N–C=O) + δ(C–N–H) + aromatic ring stretch
1633	1661	ν(C–N) + aromatic ring stretch

ν, stretching; δ, in-plane deformation; ρ, rocking; as, asymmetric

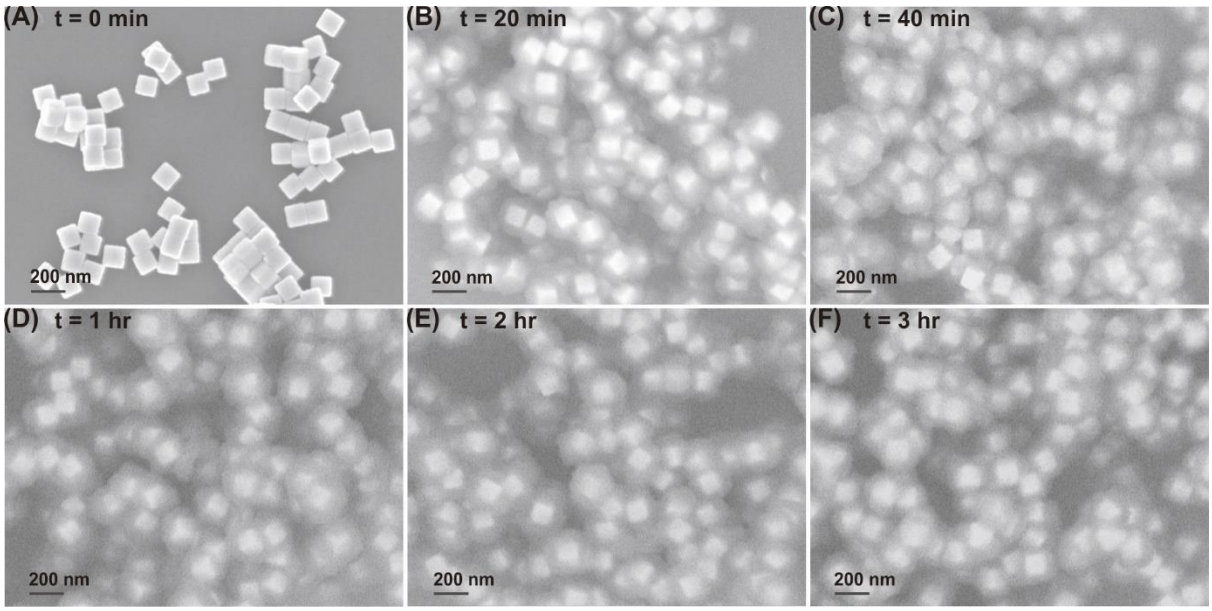

Figure S10. SEM characterization in the optimization of ZIF coating onto Ag nanocubes for the formation of Ag@ZIF nanocubes (A) 0 min, (B) 20 min, (C) 40 min, (D) 1 hour, (E) 2 hour, (F) 3 hour, respectively.

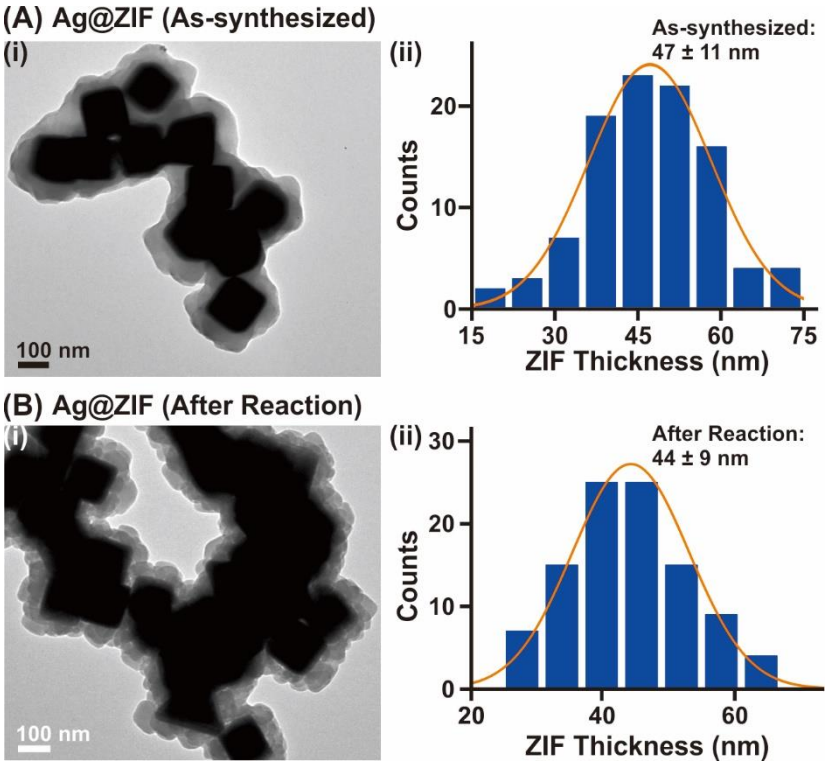

Figure S11. Characterization of Ag@ZIF nanocubes. (A) As-synthesized Ag@ZIF nanocubes and (B) activated Ag@ZIF after reaction. (i) TEM image and (ii) ZIF thickness distribution.

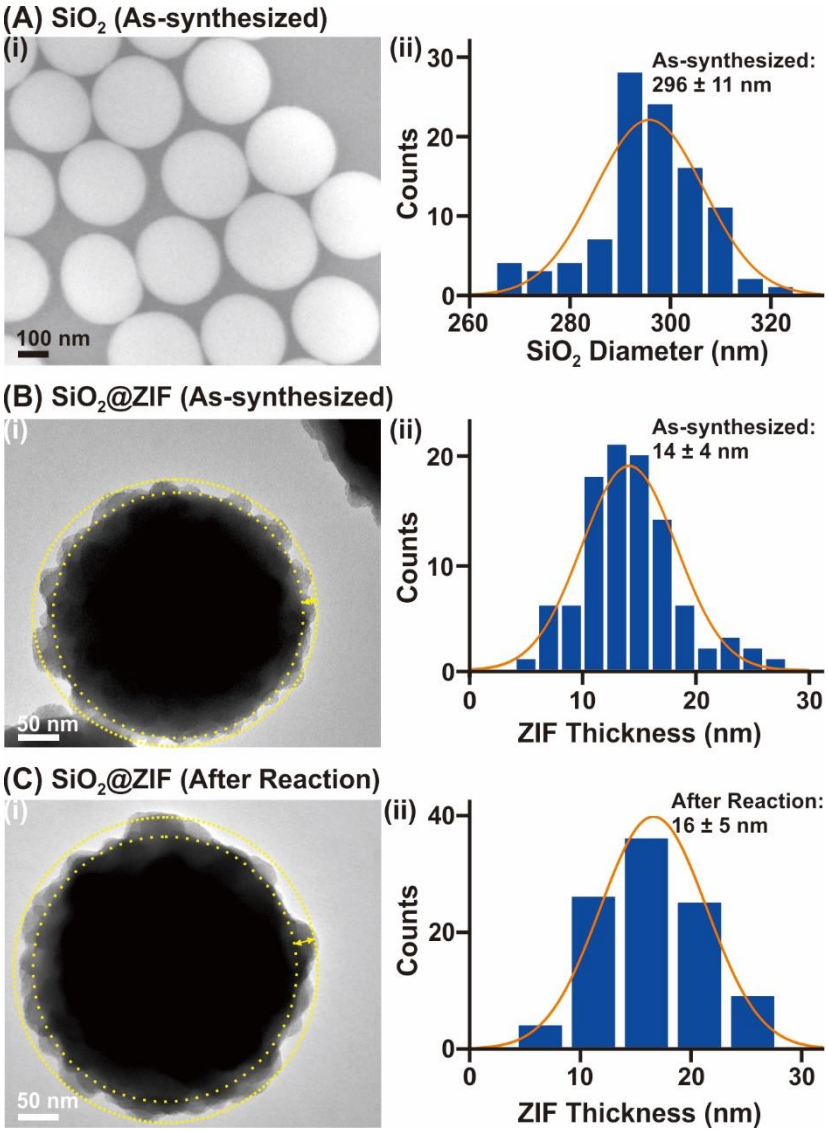

Figure S12. Characterization of SiO_2 and SiO_2@ZIF nanoparticles. (A) As-synthesized SiO_2 nanoparticles. (i) SEM image and (ii) particle diameter distribution. (B) As-synthesized SiO_2@ZIF and (C) activated SiO_2@ZIF after reaction. (i) TEM image and (ii) ZIF thickness distribution.

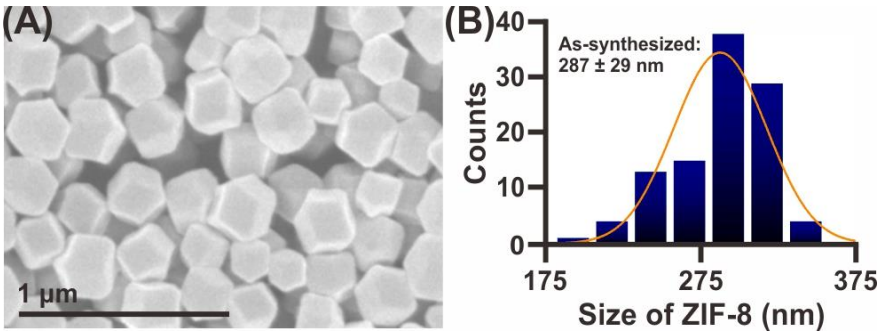

Figure S13. Characterization of ZIF particles. (A) SEM image and (B) size distribution of ZIF particles.

Our as-synthesized ZIF particles exhibit an average particle size of 287 ± 29 nm (Figure S13), which is slightly bigger compared to the overall size of our Ag@ZIF particles (221 ± 16 nm; Figure S11). Nevertheless, we have considered the size of ZIF particles by normalizing all reaction efficiency against ZIF's mass to ensure fair reaction rate comparison. This is because the amount of ZIF present could potentially impact the gas sorption capability of Ag@ZIF.

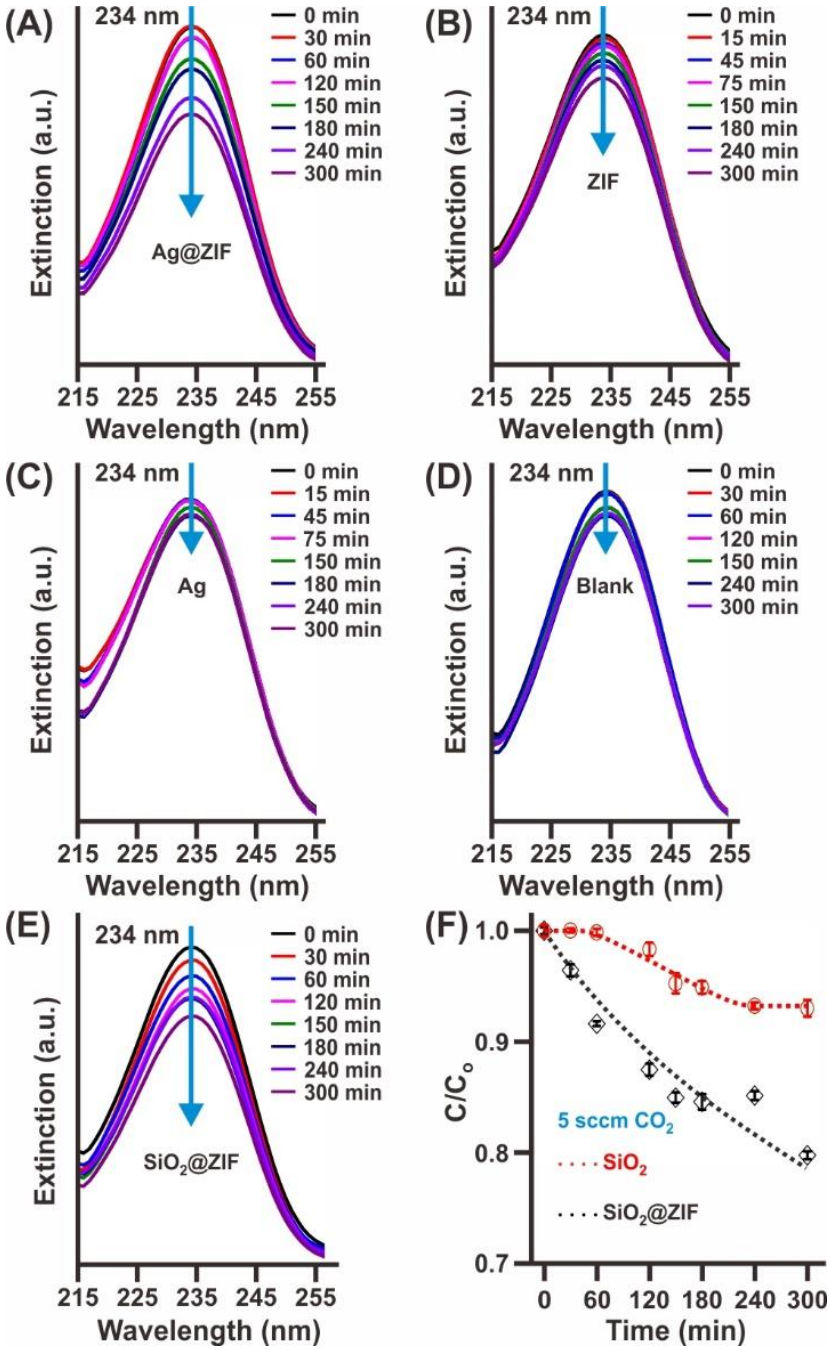

Figure S14. Monitoring gas-liquid reaction using temporal UV-Vis absorption measurement. UV-Vis absorption spectra of respective reaction setups involving (A) Ag@ZIF, (B) ZIF only, (C) Ag only, (D) blank and (E) SiO_2@ZIF. (F) C/C_0 plot of reaction setups involving SiO_2@ZIF and SiO_2. All gas-liquid reactions are performed at a CO_2 flow rate of 5 sccm.

SUPPORTING INFORMATION

Supporting Text 1 (Calculation on the mass of aniline consume per mass of ZIF)

For Ag@ZIF

We estimate the mass of ZIF in a Ag@ZIF nanoparticle by assuming that the ZIF layer conformally coats the entire Ag nanocube (AgNC). Hence, the volume of Ag@ZIF can be determined as followed:

Volume $_{Ag@ZIF}$ = (Length $_{Ag@ZIF}$)^3

= (221.1 nm)^3

= 1.08 × 10^7 nm^3

= 1.08 × 10^{-14} cm^3

Volume $_{Ag}$ = (Length $_{Ag}$)^3

= (126.7 nm)^3

= 2.03 × 10^6 nm^3

= 2.03 × 10^{-15} cm^3

Volume $_{ZIF}$ = Volume $_{Ag@ZIF}$ - Volume $_{Ag}$

= (1.08 × 10^{-14} - 2.03 × 10^{-15}) cm^3

= 8.77 × 10^{-15} cm^3

Mass $_{ZIF}$ = Density $_{ZIF}$ × Volume $_{ZIF}$

= 0.3 g cm^{-3} × 8.77 × 10^{-15} cm^3

= 2.63 × 10^{-15} g

Mass $_{Ag}$ = Density $_{Ag}$ × Volume $_{Ag}$

= 10.49 g cm^{-3} × 2.03 × 10^{-15} cm^3

= 2.13 × 10^{-14} g

Given that the total mass of Ag@ZIF used = 2 mg

$$\text{Mass}_{ZIF} \text{ in Ag@ZIF} = \frac{\text{Mass}_{ZIF}}{\text{Mass}_{Ag}+\text{Mass}_{ZIF}} \times 2 \text{ mg}$$

$$= \frac{2.63 \times 10^{-15}}{2.13 \times 10^{-14} + 2.63 \times 10^{-15}} \times 2 \text{ mg}$$

= 0.22 mg

From the extinction spectra obtained, C/C_o of aniline at t = 300 min is quantified to be 0.765 which denotes that 23.5 % of aniline has been consumed. By benchmarking against blank control experiment, the effective consumption of aniline in Ag@ZIF is calculated to be 17.4 %. Since the initial aniline concentration is 0.1 M, the mass of aniline consumed during the reaction duration of 300 min is estimated as followed:

Mass $_{aniline}$ = Volume $_{aniline}$ × Initial Concentration $_{aniline}$ × Molecular Weight $_{aniline}$ × % effective aniline consumed

= 1.3 × 10^{-3} L × 0.1 M × 93.13 g mol^{-1} × 17.4 % × 1000

= 2.11 mg

Mass $_{Aniline}$ consumption normalized with Mass $_{ZIF}$ = (2.11 mg $_{aniline}$ ÷ 0.22 mg $_{ZIF}$)

= 9.6 mg $_{aniline}$ mg $_{ZIF}^{-1}$

SUPPORTING INFORMATION

For ZIF only

From the extinction spectra obtained, C/C_o of aniline at t = 300 min is quantified to be 0.883 which denotes that 11.7 % of aniline has been consumed. By benchmarking against blank control experiment, the effective consumption of aniline in ZIF is calculated to be 5.7 %. Since the initial aniline concentration is 0.1 M, the mass of aniline consumed during the reaction duration of 300 min is estimated as followed:

$$\text{Mass}_{\text{aniline}} = \text{Volume}_{\text{aniline}} \times \text{Initial Concentration}_{\text{aniline}} \times \text{Molecular Weight}_{\text{aniline}} \times \% \text{ effective aniline consumed}$$

$$= 1.3 \times 10^{-3}\ \text{L} \times 0.1\ \text{M} \times 93.13\ \text{g mol}^{-1} \times 5.7\ \% \times 1000$$

$$= 0.686\ \text{mg}$$

$$\text{Mass}_{\text{Aniline}} \text{ consumption normalized with Mass}_{\text{ZIF}} = (0.686\ \text{mg}_{\text{aniline}} \div 2\ \text{mg}_{\text{ZIF}})$$

$$= 0.343\ \text{mg}_{\text{aniline}}\ \text{mg}_{\text{ZIF}}^{-1}$$

SUPPORTING INFORMATION

Supporting Text 2 (Calculation on the mass of aniline consumed per mass of ZIF and per interfacial area)

For Ag@ZIF

Based on the calculation achieved in Supporting Text 1 for Ag@ZIF, we further normalized it with the interfacial area by assuming that interfacial area is approximately the total surface area of cube surface.

Interfacial Area $_{Ag}$ = 6 × (0.1267 μm)^2

= 9.62 × 10^{-2} μm^2

Mass $_{Aniline}$ consumption normalized with Mass $_{ZIF}$ and Mass $_{interfacial\ area}$

= 2.11 mg ÷ [0.22 mg × 9.62 × 10^{-2} μm^2]

= 99.7 mg $_{aniline}$ mg $_{ZIF}^{-1}$ μm $_{interfacial\ area}^{-2}$

For SiO_2@ZIF

We estimate the mass of ZIF in a SiO_2@ZIF nanoparticle by assuming that the ZIF layer conformally coats the entire SiO_2 nanosphere. Hence, the volume of SiO_2@ZIF can be determined as followed:

Volume $_{SiO2@ZIF}$ = (4/3) π (Radius $_{SiO2@ZIF}$)^3

= (4/3) π (162 nm)^3

= 1.78 × 10^7 nm^3

= 1.78 × 10^{-14} cm^3

Volume $_{SiO2}$ = (4/3) π (Radius $_{SiO2}$)^3

= (4/3) π (148 nm)^3

= 1.36 × 10^7 nm^3

= 1.36 × 10^{-14} cm^3

Volume $_{ZIF}$ = Volume $_{SiO2@ZIF}$ - Volume $_{SiO2}$

= (1.78 × 10^{-14} - 1.36 × 10^{-14}) cm^3

= 4.25 × 10^{-15} cm^3

Mass $_{ZIF}$ = Density $_{ZIF}$ × Volume $_{ZIF}$

= 0.3 g cm^{-3} × 4.25 × 10^{-15} cm^3

= 1.28 × 10^{-15} g

Mass $_{SiO2}$ = Density $_{SiO2}$ × Volume $_{SiO2}$

= 2.65 g cm^{-3} × 1.36 × 10^{-14} cm^3

= 3.59 × 10^{-14} g

Given that the total mass of SiO_2@ZIF used = 2 mg

Mass $_{ZIF}$ in SiO_2@ZIF = $\frac{\text{Mass}_{\text{ZIF}}}{\text{Mass}_{\text{SiO}_2}+\text{Mass}_{\text{ZIF}}} \times 2$ mg

= $\frac{1.28 \times 10^{-15}}{3.59 \times 10^{-14} + 1.28 \times 10^{-15}} \times 2$ mg

= 0.069 mg

SUPPORTING INFORMATION

From the extinction spectra obtained, C/C_o of aniline at t = 300 min is quantified to be 0.8 which denotes that 20 % of aniline has been consumed. By benchmarking against blank control experiment, the effective consumption of aniline in SiO_2@ZIF is calculated to be 14.2 %. Since the initial aniline concentration is 0.1 M, the mass of aniline consumed during the reaction duration of 300 min is estimated as followed:

$\text{Mass}_{\text{aniline}} = \text{Volume}_{\text{aniline}} \times \text{Initial Concentration}_{\text{aniline}} \times \text{Molecular Weight}_{\text{aniline}} \times \%\ \text{effective aniline consumed}$

$= 1.3 \times 10^{-3}\ \text{L} \times 0.1\ \text{M} \times 93.13\ \text{g mol}^{-1} \times 14.2\ \% \times 1000$

$= 1.71\ \text{mg}$

We normalized the aniline consumption with the mass of ZIF and the interfacial area by assuming that interfacial area is approximately the total surface area of sphere surface.

$\text{Interfacial Area}_{SiO2} = (4\pi)\ (\text{Radius}_{SiO2})^2$

$= 4\pi \times (0.148\ \mu\text{m})^2$

$= 0.275\ \mu\text{m}^2$

$\text{Mass}_{\text{Aniline}}$ consumption normalized with Mass_{ZIF} and $\text{Mass}_{\text{interfacial area}}$

$= 1.71\ \text{mg} \div [0.069\ \text{mg} \times 0.275\ \mu\text{m}^2]$

$= 90.9\ \text{mg}_{\text{aniline}}\ \text{mg}_{\text{ZIF}}^{-1}\ \mu\text{m}_{\text{interfacial area}}^{-2}$

References

1. Lee, H. K.; Lee, Y. H.; Phang, I. Y.; Wei, J.; Miao. Y. E.; Liu, T.; Ling, X. Y. *Angew. Chem., Int. Ed.* **2014,** *53*, 5054.
2. Koh, C. S. L.; Lee, H. K.; Han, X.; Sim, H. Y. F.; Ling, X. Y. *Chem. Commun.* **2018,** *54*, 2546.
3. Lu, G.; Hupp, J. T. *J. Am. Chem. Soc.* **2010,** *132*, 7832.
4. You, T. T.; Yin, P. G.; Jiang, L.; Lang, X. F.; Guo, L.; Yang, S. H. *Phys. Chem. Chem. Phys.* **2012,** *14*, 6817.
5. Zhang, W.; Lu, G.; Li, S.; Liu, Y.; Xu, H.; Cui, C.; Yan, W.; Yang, Y.; Huo, F. *Chem. Commun.* **2014**, *50*, 4296.
6. Zhou, X.; Huang, X.; Qi, X.; Wu, S.; Xue, C.; Boey, F. Y. C.; Yan, Q.; Chen, P.; Zhang, H. *J. Phys. Chem. C* **2009**, *113*, 10842.
7. Lee, H. K.; Lee, Y. H.; Morabito, J. V.; Liu, Y.; Koh, C. S. L.; Phang, I. Y.; Pedireddy, S.; Han, X.; Chou, L.Y.; Tsung, C. K.; Ling, X. Y. *J. Am. Chem. Soc.* **2017**, *139*, 11513
8. Borjigin, T.; Sun, F.; Zhang, J.; Cai, K.; Ren, H.; Zhu, G. *Chem. Commun.* **2012,** *48*, 7613.
9. Anasthasiya, A. N. A.; Kampara, R. K.; Rai, P. K.; Jeyaprakash, B. G. *Appl. Surf. Sci.* **2018,** *449*, 244.
10. Mammone, J. F.; Sharma, S. K.; Nicol, M. *J. Phys. Chem.* **1980,** *84*, 3130.
11. Qi, Y.; Hu, Y.; Xie, Min.; Xing, D.; Gu, H. *J. Raman Spectrosc.* **2011,** *42*, 1287.
12. Laurentius, L.; Stoyanov, S. R.; Gusarov, S.; Kovalenko, A.; Du, R.; Lopinski, G. P.; McDermott, M. T. *ACS Nano* **2011,** *5*, 4219.
13. Han, X.; Lee, H. K.; Lee, Y. H.; Hao, W.; Liu, Y.; Phang, I. Y.; Li, S.; Ling, X. Y. *J. Phys. Chem. Lett.* **2016,** *7*, 1501.